AIMS Biophysics

AIMS Biophysics, 10(1): 121–131.
DOI: 10.3934/biophy.2023009
Received: 19 October 2022
Revised: 30 January 2023
Accepted: 21 February 2023
Published: 23 March 2023

http://www.aimspress.com/journal/biophysics

Research article

Natural bond orbital analysis of dication magnesium complexes $[Mg(H_2O)_6]^{2+}$ and $[[Mg(H_2O)_6](H_2O)_n]^{2+}$; n=1-4

Ganesh Prasad Tiwari[1], Santosh Adhikari[1], Hari Prasad Lamichhane[2] and Dinesh Kumar Chaudhary[1,2,*]

[1] Department of Physics, Amrit Campus, Tribhuvan University, Kathmandu 44600, Nepal
[2] Central Department of Physics, Tribhuvan University, Kirtipur, Kathmandu 44618, Nepal

* **Correspondence:** Email: dinesh.chaudhary@ac.tu.edu.np; Tel: +977984128616.

Abstract: The metal ion is ubiquitous in the human body and is essential to biochemical reactions. The study of the metal ion complexes and their charge transfer nature will be fruitful for drug design and may be beneficial for the extension of the field. In this regard, investigations into charge transport properties from ligands to metal ion complexes and their stability are crucial in the medical field. In this work, the DFT technique has been applied to analyze the delocalization of electrons from the water ligands to a core metal ion. At the B3LYP level of approximation, natural bond orbital (NBO) analysis was performed for the first five distinct complexes $[Mg(H_2O)_6]^{2+}$ and $[[Mg(H_2O)_6](H_2O)_n]^{2+}$; n = 1-4. All these complexes were optimized and examined with the higher basis set 6-311++G(d, p). In the complex $[Mg(H_2O)_6]^{2+}$, the amount of natural charge transport from ligands towards the metal ion was 0.179e, and the greatest stabilization energy was observed to be 22.67 kcal/mol. The donation of the p orbitals in the hybrid orbitals was increased while approaching the oxygen atoms of H_2O ligands in the 1st coordination sphere with the magnesium ions. The presence of water ligands within the 2nd coordination sphere increased natural charge transfer and decreased the stabilizing energy of the complexes. This may be due to the ligand-metal interactions.

Keywords: DFT; B3LYP; delocalization; NBO; Ligand; dication

1. Introduction

Dication magnesium complexes have a unique place in chemistry and biochemistry due to their

diverse structural arrangements and applications in numerous fields. Magnesium is very crucial for living beings. For example, about 300 metabolic activities and 800 proteins require this metal to function in our body. This metal is also necessary for DNA [1,2], RNA [3,4], antioxidant glutathione production [5], energy generation, oxidative phosphorylation, and glycolysis among other elements, helps the anatomical formation of bone, with exterior layers assisting in the maintenance of blood magnesium levels [6], while magnesium shortage has been associated with decreased bone mass [7,8]. In plants, Chlorophyll, a magnesium coordination molecule, is required for plant life (Photosynthesis) and the survival of life on Earth [9,10]. Magnesium also participates in active Ca and K ion transport across cell membranes, which are required for nerve impulse transmission, muscle contraction, and a regular heart rhythm [11,12].

Computational chemistry has recently acquired popularity among scholars and researchers as a method of addressing real-world challenges in chemical, pharmaceutical, biotechnology, and material science [13]. By Bock *et al.*, the stereochemistry of ligand binding by bivalent magnesium metal was effectively analyzed, as was how likely these ligands are to be water [14]. Ab initio molecular orbital (MO) calculation of $M^{2+}(H_2O)_n$ complexes having central alkaline earth metal ion with varying water ligands from one to six at RHF and MP2 level with basis set 6-31+G* was investigated by Glendening *et al.* [15]. The alkaline-earth metal ions $M^{2+}(H_2O)_n$, n = 5-7 (M = Mg, Ca, Sr, and Ba) hydration energies and geometries were determined by Rodriguez-Cruz *et al.* [16] using the DFT-B3LYP method. According to Pavlov *et al.* [17], charge transfer between the ligands and the metal lowers the interaction energy of the complex $[Mg(H_2O)_n]^{2+}$ between M···H_2O as the number of ligands rises in the 2nd coordination sphere. By employing the kinetic energy release measurement method, Bruzzi *et al.* [18] investigated the binding energies of complexes $[Mg(NH_3)_n]^{2+}$, $[Ca(NH_3)_n]^{2+}$, and $[Sr(NH_3)_n]^{2+}$ for n = 4–20, and these results are supported by DFT calculations. These desired impacts have provided new insights into the trustworthiness of computational methodologies.

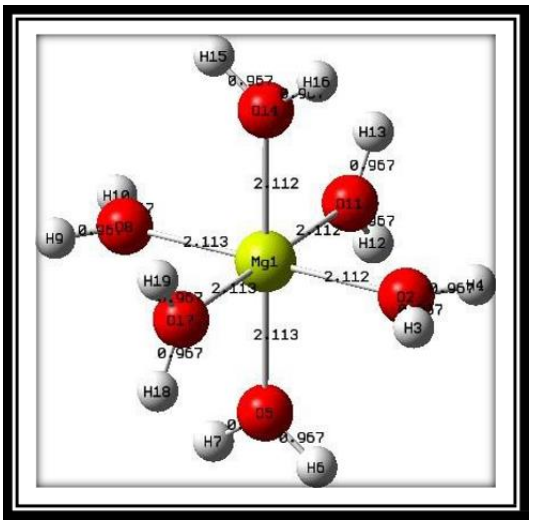

Figure 1. Structural representation of the octahedral magnesium complex $[Mg(H_2O)_6]^{2+}$ showing bond lengths.

Several preceding studies reveal the focus on the coordinative behavior of metal ions however, the natural bond orbital analysis of metal complexes by using the DFT-B3LYP approach with varying numbers of ligands in 2nd coordination sphere is yet to be studied. The charge transfer from

surrounding ligands to a central metal ion and vice versa affects its geometry and other physical features of complexes. Two charge transfer mechanisms, Mulliken and natural, are explained by population analysis. NBO analysis provides a solid framework for researching charge transfer and conjugative interactions in atoms and molecules. The second-order perturbation hypothesis leads to the availability of some electron donor orbitals, acceptor orbitals, and association stabilization energies [19]. The system conjugation increases with increasing $E^{(2)}$ value and electron donor interaction. When electron density delocalizes between occupied Lewis type (bond or lone pair) and nominally vacant non-Lewis type (antibonding or Rydberg) NBO orbitals, a stable donor-acceptor interaction is ensured [17]. The natural bond orbital study of magnesium compounds using the DFT-B3LYP approach with varying quantities of ligands in 2nd coordination sphere remains unexplored. This work reports the study of natural transfer properties in the coordination complex $[Mg(H_2O)_6]^{2+}$. Figure 1 illustrates the optimized structural representation of complex $[Mg(H_2O)_6]^{2+}$ that displays bond lengths. The central metal ion is attached to identical six water ligands, forming an octahedral structure. The distance between Mg and O is 2.112 Å, while the distance between O and H is 0.967Å. The remaining four complexes were created by gradually expanding the number of water molecules within 2nd coordination sphere from one to four. Natural charge transfer behavior of the different complexes was then compared. This study of magnesium complexes will shed light on the charge transfer behavior of metal ions. The analysis of these complexes will be beneficial for medicinal design and could aid in the development of new drugs.

2. Materials and methods

The quantum computations in this extensive analysis of metal complexes were accomplished with the Gaussian 16 program packages [20]. Gaussian inputs of magnesium ion compounds were generated, and outputs were displayed using GaussView 6 [21]. The structural geometrics of complexes were firstly optimized utilizing various basis sets with B3LYP functional, which combines Becke's gradient-correlated exchange functional (B3) [22] and Lee-Yang-Parr (LYP) [23]. These inputs were acquired by retaining the ligands in a quasi-octahedral structure. There was no symmetry limitation enforced, and the C_1 point group symmetry was used for optimization. Frequency estimations were carried out during the geometry optimization process, and global minima were validated. Every calculation was carried out by applying 6-311++G(d,p) basis set and B3LYP functional. NBOs provide precise details on the type of electronic conjugation occurring between molecular bonds. In metal complexes, the delocalization of electrons results once the hybridized orbitals of water molecules and metal ions coincides. NBO evaluation is a strong approach for determining this electron delocalization. NBOs strongly support the assumption that localized bonds and lone pairs are the essential building blocks of molecular structure, hence it is feasible to understand ab initio wave functions in perspective of Lewis structure theories by effectively converting them to NBO form. The NBO technique was utilized to study how the non-bonding pairs of oxygen atoms in the water decreased their native charge densities. NBO analysis is performed by looking at all conceivable interactions between 'full' (donor) Lewis-type NBOs and 'empty' (acceptor) non-Lewis NBOs and evaluating their energetic significance using second-order perturbation theory. Since these exchanges result in the transfer of occupancy from the idealized Lewis structure's localized NBOs into the unoccupied non-Lewis orbitals (and hence deviations from the idealized Lewis structure description), they are termed to as "delocalization" corrections to the zeroth-order natural Lewis

structure [23]. This work presents the outcomes of a second-order perturbation theory investigation of the Fock matrix within the NBO of the complexes. The delocalization-related stabilizing energy $E^{(2)}$ for each donating NBO (i) and receiver NBO (j) is determined as

$$E^{(2)} = q_i \frac{< i|\hat{F}|j >}{\epsilon_i - \epsilon_j}$$

where q_i stands for orbital occupancy of a donor, ϵ_i, ϵ_j represents orbital energies, and F(i,j) for the off-diagonal NBO Fock matrix component [24]. Higher value of stabilization energy $E^{(2)}$ denotes powerful interaction between acceptors and donors [25].

3. Results and discussion

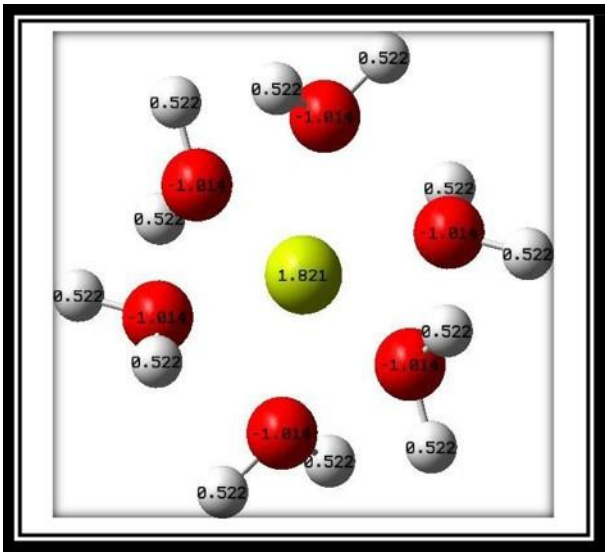

Figure 2. Natural charges on constituent atoms in the complex $[Mg(H_2O)_6]^{2+}$.

Table 1. Natural charges on the central metal ion Mg^Q and ligands to metal charge transfer ΔQ in the complexes $[[Mg(H_2O)_6](H_2O)_n]^{2+}$; n = 0-4.

Complex	Mg^Q(e)	ΔQ(e)
$[Mg(H_2O)_6]^{2+}$	1.821	0.179
$[[Mg(H_2O)_6](H_2O)]^{2+}$	1.820	0.180
$[[Mg(H_2O)_6](H_2O)_2]^{2+}$	1.819	0.181
$[[Mg(H_2O)_6](H_2O)_3]^{2+}$	1.818	0.182
$[[Mg(H_2O)_6](H_2O)_4]^{2+}$	1.817	0.183

The natural charges on the central metal ion Mg^{2+} and charge transfer in the complexes $[[Mg(H_2O)_6](H_2O)_n]^{2+}$; n = 0-4 are demonstrated in Table 1. The charge transfer takes place in all complexes. The NBO partial charge on metal ions does not widely vary when the number of molecules within the 2nd coordination sphere is increased, but there are modest increases, as shown in Table 1. Figure 2 depicts the octahedral structural representation of complex $[Mg(H_2O)_6]^{2+}$ with natural charges

on constituent atoms. This central metal ion is surrounded by six identical water molecules in the 1st coordination sphere. The total charge constituent in the whole complex equals +2e. Figure 3(a) shows the representation of the complex when one water ligand is added to its 2nd coordination sphere. Likewise, Figure 3(b), Figure 3(c), and Figure 3(d) represent the figurative representatives of complexes after the addition of two, three, and four water ligands to their 2nd coordination sphere, respectively. The total electron density of the $[Mg(H_2O)_6]^{2+}$ is used to express the overall effectiveness of the natural Lewis structure analysis as a percentage. Table 2 demonstrates the importance of valance non-Lewis orbitals in comparison to extra-valence electron shells in modest deviations from a confined Lewis structure model.

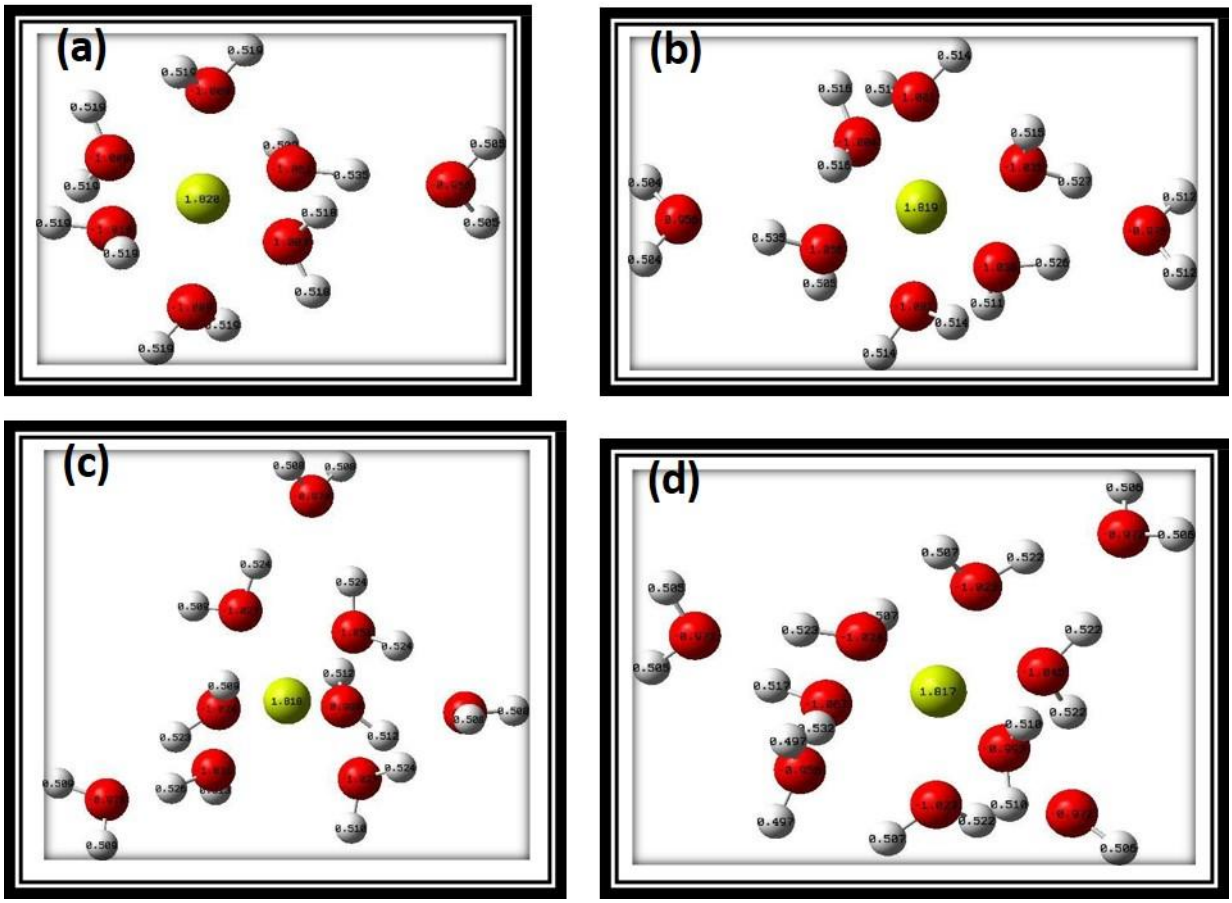

Figure 3. The natural charges on constituent atoms in the complex (a) $[[Mg(H_2O)_6](H_2O)]^{2+}$, (b) $[[Mg(H_2O)_6](H_2O)_2]^{2+}$, (c) $[[Mg(H_2O)_6](H_2O)_3]^{2+}$, and (d) $[[Mg(H_2O)_6](H_2O)_4]^{2+}$ with extension of one to four ligands in the 2nd coordination sphere respectively.

Table 2. Separation of Lewis and non-Lewis occupancies within complex $[Mg(H_2O)_6]^{2+}$ into core, valence, and Rydberg shell components.

Orbitals	Occupancy
Core	21.99748 (99.989% of 22)
Valence Lewis	47.77540 (99.532% of 48)
Total Lewis	69.77288 (99.676% of 70)
Valence non-Lewis	0.18649 (0.266% of 70)
Rydberg non-Lewis	0.04063 (0.058% of 70)
Total non-Lewis	0.22712 (0.324% of 70)

The electron delocalization through lone pairs of oxygen to iron orbitals was evaluated. The table below shows the two most powerful interactions. The interchange of non-bonding pairs of oxygen with metal $n*$ orbitals is determined to be greatest in the instance of a complex $[Mg(H_2O)_6]^{2+}$. The greatest interaction in the complex is likewise demonstrated to be between metal orbitals and virtual orbitals.

Table 3. Result of second-order perturbation theory evaluation of Fock matrix within NBO of complex $[Mg(H_2O)_6]^{2+}$.

Donor NBOs	Occupancy (e)	Hybrid (%)	Acceptor NBOs	Occupancy (e)	Hybrid (%)	$E^{(2)}$ (kcal/mol)
LP O (2)	1.96849	$s^{47.65}p^{52.34}$	LP* Mg	0.17178	s^{100}	22.67
LP O (5)	1.96853	$s^{47.66}p^{52.34}$	LP* Mg	0.17178	s^{100}	22.63
LP O (8)	1.96853	$s^{47.65}p^{52.34}$	LP* Mg	0.17178	s^{100}	22.63
LP O (11)	1.96851	$s^{47.66}p^{52.34}$	LP* Mg	0.17178	s^{100}	22.66
LP O (14)	1.96849	$s^{47.65}p^{52.34}$	LP* Mg	0.17178	s^{100}	22.67
LP O (17)	1.96854	$s^{47.66}p^{52.34}$	LP* Mg	0.17178	s^{100}	22.62

From Table 3, it is seen that delocalization of oxygen lone pairs to $n*$ orbitals of Mg^{2+} occurred in the stronger interactions of LP O (2) and LP O (14) with LP* Mg with occupancy of 0.17178e stabilizes $[Mg(H_2O)_6]^{2+}$ complex by 22.67 kcal/mol. These stabilization energies of complexes are balanced by the remaining stabilization energies of complexes. This analysis reveals that, on the donor orbital side, the p orbital contributes more than the s orbital, whereas the d orbital does not contribute. On the acceptor side, the contribution of the p and d orbitals was negligible in comparison to the s orbital for the maximum stabilization energy. In a few cases of acceptor orbitals, the contribution of the p orbital and d orbital is also seen. The greatest stabilization energy of complex $[Mg(H_2O)_6]^{2+}$ is less than that of the complex $[Zn(H_2O)_6]^{2+}$ as reported by Pokharel et al. [26].

The NBO partial charge on the metal ions does not change much on adding the number of ligands within the 2nd coordination sphere. It displays some findings from an investigation into the Fock matrix within the NBO of complexes by utilizing second-order perturbation analysis. Only the interaction resulting from the delocalization of the electrons from the oxygen lone pairs of ligands in the 1st coordination sphere to the $n*$ orbitals of Mg^{2+} was obtained to have stabilization energies of more than 5 kcal/mol in all circumstances. As a result, these tables only include the most powerful interactions. The powerful interaction among the associated interactions is one in which electrons from non-binding pairs of O (2) are delocalized to the LP* Mg with occupancy 0.17343e, as shown in Table 4. This is the interaction when

one water ligand is attached within the 2nd coordination sphere of a complex $[Mg(H_2O)_6]^{2+}$. As shown by the preceding result, the bond between magnesium and oxygen has been shortened compared to that of the complex $[Mg(H_2O)_6]^{2+}$ because of the presence of one water ligand in the 2nd coordination sphere.

Table 4. Result of second-order perturbation theory evaluation of matrix within NBO of the complex $[[Mg(H_2O)_6](H_2O)]^{2+}$.

Donor NBOs	Occupancy (e)	Hybrid (%)	Acceptor NBOs	Occupancy (e)	Hybrid (%)	$E^{(2)}$ (kcal/mol)
LP O (2)	1.96238	s43.80p56.20	LP* Mg	0.17343	s100	25.47
LP O (5)	1.96938	s47.66p52.34	LP* Mg	0.17343	s100	22.38
LP O (8)	1.96955	s47.65p52.35	LP* Mg	0.17343	s100	22.06
LP O (11)	1.96874	s46.67p53.32	LP* Mg	0.17343	s100	22.51
LP O (14)	1.96938	s47.66p52.34	LP* Mg	0.17343	s100	22.37
LP O (17)	1.96967	s47.74p52.25	LP* Mg	0.17343	s100	22.15

Table 5. Result of second-order perturbation theory evaluation of Fock matrix within NBO of the complex $[[Mg(H_2O)_6](H_2O)_2]^{2+}$.

Donor NBOs	Occupancy (e)	Hybrid (%)	Acceptor NBOs	Occupancy (e)	Hybrid (%)	$E^{(2)}$ (kcal/mol)
LP O (2)	1.96371	$s^{44.71}p^{55.79}$	LP* Mg	0.17413	$s^{99.99}p^{0.01}$	24.64
LP O (5)	1.97016	$s^{46.32}p^{53.67}$	LP* Mg	0.17413	$s^{99.99}p^{0.01}$	24.71
LP O (8)	1.96726	$s^{44.71}p^{55.28}$	LP* Mg	0.17413	$s^{99.99}p^{0.01}$	22.82
LP O (11)	1.97003	$s^{46.70}p^{53.29}$	LP* Mg	0.17413	$s^{99.99}p^{0.01}$	21.86
LP O (14)	1.97015	$s^{46.34}p^{53.66}$	LP* Mg	0.17413	$s^{99.99}p^{0.01}$	21.74
LP O (17)	1.96663	$s^{45.22}p^{54.77}$	LP* Mg	0.17413	$s^{99.99}p^{0.01}$	23.47

Table 5 shows two strong $E^{(2)}$ that are near to one another. One is from the delocalization of electrons from non-bonding pairs of O (5) and another is from O (2) to the LP* Mg having occupancy 0.17413e with stabilization energies of 24.71 kcal/mol and 24.64 kcal/mol respectively.

In a complex $[[Mg(H_2O)_6](H_2O)_3]^{2+}$, the most powerful engagement is because of the delocalization of the electrons from non-bonding pairs of O (2) to LP* Mg with occupancy 0.17514e that balanced this ion by 24.09 kcal/mol. Moreover, the other two nearly equal interactions are seen because of the delocalization of non-bonding pairs of O (8) and O (17) with LP* Mg having stabilization energy of 23.06 kcal/mol and 23.13 kcal/mol respectively. The powerful interactions are presented in Table 6.

Table 6. Result of second-order perturbation theory evaluation of Fock matrix within NBO of the complex $[[Mg(H_2O)_6](H_2O)_3]^{2+}$.

Donor NBOs	Occupancy (e)	Hybrid (%)	Acceptor NBOs	Occupancy (e)	Hybrid (%)	$E^{(2)}$ (kcal/mol)
LP O (2)	1.96511	$s^{41.70}p^{58.30}d^{0.00}$	LP* Mg	0.17514	$s^{99.99}p^{0.01}$	24.09
LP O (5)	1.96762	$s^{43.30}p^{56.70}d^{0.01}$	LP* Mg	0.17514	$s^{99.99}p^{0.01}$	22.55
LP O (8)	1.96754	$s^{44.71}p^{55.29}d^{0.01}$	LP* Mg	0.17514	$s^{99.99}p^{0.01}$	23.06
LPO (11)	1.97130	$s^{46.77}p^{53.23}d^{0.01}$	LP* Mg	0.17514	$s^{99.99}p^{0.01}$	21.21
LPO (14)	1.96764	$s^{43.23}p^{56.76}d^{0.01}$	LP* Mg	0.17514	$s^{99.99}p^{0.01}$	22.57
LP O (17)	1.96763	$s^{45.06}p^{54.94}d^{0.00}$	LP* Mg	0.17514	$s^{99.99}p^{0.01}$	23.13

Lastly, in Table 7, the greatest interactions among strong interactions are because of the delocalization of the electrons from the non-bonding pairs of O (8) with LP* Mg having occupancy of 0.17653e by stabilization energies of 25.21 kcal/mol. The stabilization energies of the remaining three interactions, which are strong, are 23.13 kcal/mol, 22.92 kcal/mol, and 22.16 kcal/mol.

Table 7. Result of second-order perturbation theory evaluation of Fock matrix within NBO of the complex $[[Mg(H_2O)_6](H_2O)_4]^{2+}$.

Donor NBOs	Occupancy (e)	Hybrid (%)	Acceptor NBOs	Occupancy (e)	Hybrid (%)	$E^{(2)}$ (kcal/mol)
LP O (2)	1.96618	$s^{41.20}p^{58.80}d^{0.00}$	LP* Mg	0.17653	$s^{99.99}p^{0.00}d^{0.01}$	23.17
LP O (5)	1.96830	$s^{43.07}p^{56.93}d^{0.02}$	LP* Mg	0.17653	$s^{99.99}p^{0.00}d^{0.01}$	22.16
LP O (8)	1.96308	$s^{42.10}p^{57.90}d^{0.00}$	LP* Mg	0.17653	$s^{99.99}p^{0.00}d^{0.01}$	25.21
LP O (11)	1.97119	$s^{47.02}p^{52.97}d^{0.01}$	LP* Mg	0.17653	$s^{99.99}p^{0.00}d^{0.01}$	21.36
LP O (14)	1.96838	$s^{43.03}p^{56.97}d^{0.01}$	LP* Mg	0.17653	$s^{99.99}p^{0.00}d^{0.01}$	22.06
LP O (17)	1.96827	$s^{44.77}p^{55.23}d^{0.00}$	LP* Mg	0.17653	$s^{99.99}p^{0.00}d^{0.01}$	22.92

4. Conclusions

Natural charge transfer takes place between magnesium ion and the water ligands in complexes $[Mg(H_2O)_6]^{2+}$ and $[[Mg(H_2O)_6](H_2O)_n]^{2+}$; n=1-4 has been successfully studied by using NBO analysis. Among these five complexes, ligands to ion charge transfer were discovered to be greatest in complex $[[Mg(H_2O)_6](H_2O)_4]^{2+}$ and smallest in complex $[Mg(H_2O)_6]^{2+}$. The greatest stabilization energy associated with the delocalization of electrons from non-bonding pair of oxygen having LP* Mg was found to be 25.47 kcal/mol in complex $[[Mg(H_2O)_6](H_2O)_2]^{2+}$. The number of stronger interactions was observed to increase with the introduction of ligands within 2nd coordination sphere. The delocalization of electrons from non-bonding pair of oxygen in the initial coordination sphere was greater on which ligand was attached within 2nd coordination sphere than in the other oxygen lone pair. By adding more ligands to the complex's initial coordination sphere, it is possible to intensify the structures, and these intensified structures will lead to drug design.

Acknowledgments

The authors would like to thank the Department of Physics, Amrit Campus, Tribhuvan University for providing the computational laboratory for the Gaussian 16 and GaussView 6 programs to complete this work.

Conflict of interest

The authors affirm that they have no competing interest.

Author contributions

Conceptualization: Ganesh Prasad Tiwari, Hari Prasad Lamichhane, and Dinesh Kumar Chaudhary. Investigation: Ganesh Prasad Tiwari and Santosh Adhikari. Validation: Hari Prasad Lamichhane and Dinesh Kumar Chaudhary. Article writing (Original draft): Ganesh Prasad Tiwari. Writing-Review: Dinesh Kumar Chaudhary and Hari Prasad Lamichhane. All authors have read and given their consent to the final, printed version of the manuscript.

References

1. Chiu TK, Dickerson RE (2000) 1 Å crystal structures of B-DNA reveal sequence-specific binding and groove-specific bending of DNA by magnesium and calcium. *J Mol Biol* 301: 915–945. https://doi.org/10.1006/jmbi.2000.4012
2. Serra MJ, Baird JD, Dale T, et al. (2002) Effects of magnesium ions on the stabilization of RNA oligomers of defined structures. *RNA* 8: 307–323. https://doi.org/10.1017/S1355838202024226
3. Misra VK, Draper DE (1998) On the role of magnesium ions in RNA stability. *Biopolymers: Ori Res Biomol* 48: 113–135. https://doi.org/10.1002/(SICI)1097-0282(1998)48:2<113::AID-BIP3>3.0.CO;2-Y
4. Lindahl T, Adams A, Fresco JR (1966) Renaturation of transfer ribonucleic acids through site binding of magnesium. *P Natl A Sci* 55: 941–948. https://doi.org/10.1073/pnas.55.4.941
5. Mills BJ, Lindeman RD, Lang CA (1986) Magnesium deficiency inhibits biosynthesis of blood glutathione and tumor growth in the rat. *P Soc Exp Biol Med* 181: 326–332. https://doi.org/10.3181/00379727-181-42260
6. Alfrey AC, Miller NL, Trow R (1974) Effect of age and magnesium depletion on bone magnesium pools in rats. *J Clin Invest* 54: 1074–1081. https://www.jci.org/articles/view/107851
7. Rude RK, Gruber HE (2004) Magnesium deficiency and osteoporosis: animal and human observations. *J Nutr Biochem* 15: 710–716. https://doi.org/10.1016/j.jnutbio.2004.08.001
8. Rude RK, Gruber HE, Norton HJ, et al. (2004) Bone loss induced by dietary magnesium reduction to 10% of the nutrient requirement in rats is associated with increased release of substance P and tumor necrosis factor-α. *J Nutr* 134: 79–85. https://doi.org/10.1093/jn/134.1.79
9. Mohammed HS, Tripathi VD (2020) Medicinal applications of coordination complexes. *J Phys: Conf Ser* 1664: 012070. https://doi.org/10.1088/1742-6596/1664/1/012070

10. Baaij JHD, Hoenderop JG, Bindels RJ (2015) Magnesium in man: implications for health and disease. *Physiol Rev* 95: 1–46. https://journals.physiology.org/doi/full/10.1152/physrev.00012.2014
11. Schwalfenberg GK, Genuis SJ (2017) The importance of magnesium in clinical healthcare. *Scientifica* 2017: 4179326. https://doi.org/10.1155/2017/4179326
12. Sreedhara A, Cowan JA (2002) Structural and catalytic roles for divalent magnesium in nucleic acid biochemistry. *Biometals* 15: 211–223. https://doi.org/10.1023/A:1016070614042
13. Rijal R, Lamichhane HP, Pudasainee K (2022) Molecular structure, homo-lumo analysis and vibrational spectroscopy of the cancer healing pro-drug temozolomide based on dft calculations. *AIMS Biophys* 9: 208–220. https://doi.org/10.3934/biophy.2022018
14. Bock CW, Kaufman A, Glusker JP (1994) Coordination of water to magnesium cations. *Inorg Chem* 33: 419–427. https://doi.org/10.1021/ic00081a007
15. Glendening ED, Feller D (1996) Dication− Water interactions: $M^{2+}(H_2O)_n$ clusters for alkaline earth metals M= Mg, Ca, Sr, Ba, and Ra. *J Phys Chem* 100: 4790–4797. https://doi.org/10.1021/jp952546r
16. Rodriguez-Cruz SE, Jockusch RA, Williams ER (1999) Hydration energies and structures of alkaline earth metal ions, $M^{2+}(H_2O)_n$, n= 5−7, M= Mg, Ca, Sr, and Ba. *J Am Chem Soc* 121: 8898–8906. https://doi.org/10.1021/ja9911871
17. Pavlov M, Siegbahn PE, Sandström M (1998) Hydration of beryllium, magnesium, calcium, and zinc ions using density functional theory. *J Phys Chem A* 102: 219–228. https://doi.org/10.1021/jp972072r
18. Bruzzi E, Raggi G, Parajuli R, et al. (2014) Experimental binding energies for the metal complexes $[Mg(NH_3)_n]^{2+}$, $[Ca(NH_3)_n]^{2+}$, and $[Sr(NH_3)_n]^{2+}$ for n= 4–20 determined from kinetic energy release measurements. *J Phys Chem A* 118: 8525–8532. https://doi.org/10.1021/jp5022642
19. James C, Raj AA, Reghunathan R, et al. (2006) Structural conformation and vibrational spectroscopic studies of 2, 6-bis (p-N, N-dimethyl benzylidene) cyclohexanone using density functional theory. *J Raman Spectrosc* 37: 1381–1392. https://doi.org/10.1002/jrs.1554
20. Frisch MJ, Trucks GW, Schlegel HB, et al. (2016) Gaussian 16 Revision C. 01. 2016; Gaussian Inc. Wallingford CT. https://gaussian.com/gaussian16/
21. Dennington R, Keith TA, Millam JM (2019) Gaussview version 6. semichem Inc., Shawnee Mission. https://gaussian.com/gaussview6/
22. Becke A (1993) Density-functional thermochemistry.III. The role of exact exchange. *J Chem Phys* 98: 5648–5652. https://doi. org/10.1063/1.464913
23. Lee C, Yang W, Parr RG (1988) Development of the Colle-Salvetti correlation-energy formula into a functional of the electron density. *Phys Rev B* 37: 785–789. https://doi.org/10.1103/PhysRevB.37.785
24. Yogeswari B, Tamilselvan KS, Thanikaikarasan S, et al. (2022) Quantum density functional theory studies on additive hydration of tuftsin tetrapeptide. *J Nanomater* https://doi.org/10.1155/2022/2830708
25. Gangadharan RP, Krishnan SS (2014) Natural bond orbital (NBO) population analysis of 1-azanapthalene-8-ol. *Acta Phys Pol A* 125: 18–22. http://dx.doi.org/10.12693/APhysPolA.125.18

26. Pokhrel N, Lamichhane HP (2016) Natural bond orbital analysis of $[Fe(H_2O)_6]^{2+/3+}$ and $[[Zn(H_2O)_6](H_2O)_n]^{2+}$; n = 0-4. *J Phys Chem Biophys* 6: 231. http://dx.doi.org/10.4172/2161-0398.1000231

AIMS Press